



CATALYTIC PROPERTIES OF NANOSTRUCTURED METAL OXIDES SYNTHESIZED BY INERT GAS CONDENSATION

A. Tschöpe¹, D. Schaadt¹, R. Birringer¹, J.Y. Ying²

¹Universität des Saarlandes, Physik, Gebäude 43, 66041 Saarbrücken, Germany

²Massachusetts Institute of Technology, Department of Chemical Engineering, Cambridge, MA 02139, USA

Abstract -- *The correlation between defects in metal oxides and activity in heterogeneous catalytic oxidation was investigated. Processing of nanocrystalline metal oxides by inert gas condensation was employed to synthesize oxygen-deficient nonstoichiometric cerium oxide. Comparison with stoichiometric nanocrystalline ceria revealed the effect of nonstoichiometry on surface chemical reactivity. Stoichiometric nanocrystalline cerium dioxide was investigated for catalytic activity in two reactions; oxidation of CO by (i) SO₂ and (ii) O₂. Catalytic activity was found at significantly different temperatures of 560°C in the former and 360°C in the latter reaction. Complementary temperature programmed reduction (TPR) studies were performed and two distinct signals were found, which correlated with the light-off temperatures for each of the catalytic reactions. This demonstrated that the oxygen intermediates, participating in the redox mechanisms were different for both reactions. Nonstoichiometric nanocrystalline CeO_{2-x} exhibited catalytic activity in CO oxidation by O₂ and a corresponding TPR-signal at 200°C, which suggested the presence of an even more reactive oxygen species. Fourier-transform infrared spectroscopy (FT-IR) and electrical conductivity were used to study the interaction of chemisorbed CO and O₂ with the metal oxides. Surface defects and chemisorbed oxygen were discussed as possible origins of enhanced catalytic activity due to their effects on the nature of surface oxygen species. The combination of these studies yielded detailed insight into the different reaction mechanisms and the chemical interaction between solid surface and gaseous species that are critical towards the engineering of catalytic and gas sensor materials.* ©1997 Acta Metallurgica Inc.

INTRODUCTION

Catalysis is a key technology in the synthesis of chemicals and in environmental pollution control. By definition, a catalyst is a substance that increases the rate of a chemical reaction without being consumed in the process. Even if the thermodynamic driving force is given, the rate of a chemical reaction may be nearly zero due to a high activation energy. In such case, the appropriate catalyst accelerates the reaction by offering an alternative reaction path, a sequence of intermediate steps with a lower overall activation energy. In heterogeneous catalysis, these mechanisms almost always involve the chemisorption of at least one of the reactants on the surface of the catalyst. In

other words, a chemical bond between the catalyst surface and the adsorbing molecule needs to be established. The formation of a chemical bond depends decisively on the presence of unsaturated bonds at the surface. The type of bonding can be very different and may be described by well-known models such as ionosorption, or molecular-type bonding generated by an acid/base reaction etc. [1]. Nevertheless, these models all emphasize that surface defects are essential for chemisorption and hence control catalytic activity to a certain extent. The variety of possible surface sites, characterized by their degree of coordinative saturation, geometry, and the energy and symmetry of their electronic states, translates into a wide spectrum of catalytic properties. Even catalysts made of the same components may behave very differently depending on the synthesis route and pretreatment of the material.

Synthesis of nanocrystalline metal oxides in a two-step process by (i) inert gas condensation of nanometer-sized metallic clusters and (ii) post-oxidation has been reported about ten years ago [2, 3, 4]. It was commonly noticed that the resulting metal oxides were typically oxygen-deficient; for example, oxidation of nanocrystalline titanium yielded substoichiometric $\text{TiO}_{1.7}$ [4]. These kinds of materials have been investigated for catalytic properties. Beck and Siegel reported a study on the dissociative adsorption of hydrogen sulfide over nanocrystalline titanium oxide [5]. It was noticed that the materials generated by inert gas condensation exhibited higher activity than commercially available titania catalysts. This was attributed to the high surface area rutile-phase formed during synthesis. In addition, oxygen deficiency was discussed as the origin of enhanced long-term activity as this oxygen-deficient material was probably able to absorb dissociated sulfur into the lattice. Nanocrystalline Li-MgO was investigated for oxidation of methane in air and significant changes in activity as well as selectivity to higher hydrocarbons at low temperature were reported [6]. Nanocrystalline WO_{3-x} catalysts were generated by reactive evaporation of tungsten, and precious metals were deposited onto these oxide clusters [7]. Lin et al. focussed on the morphology of the resulting composite materials, thermal stability of the dispersed precious metals and the changes in catalytic activity induced by these precious metals. Nanocrystalline cerium oxide based catalysts were investigated for catalytic redox reactions such as selective catalytic reduction of sulfur dioxide by carbon monoxide to yield elemental sulfur [8, 9, 10] and catalytic oxidation of CO and methane [10]. Nonstoichiometric nanocrystalline CeO_{2-x} catalysts exhibited higher catalytic activity in all three reactions when compared to stoichiometric CeO_2 samples.

The present studies were intended to investigate the correlation between defects in metal oxides and catalytic properties. Two catalytic oxidation reactions were investigated; the oxidation of CO by (i) SO_2 and (ii) O_2 . Catalytic activation temperatures were compared with results from complementary studies. Temperature programmed reduction (TPR) was used to characterize the chemical reactivity of lattice and surface oxygen present in the metal oxide samples. The nature of carbon monoxide chemisorbed on cerium oxide was investigated by *in situ* Fourier-transform infrared spectroscopy (FT-IR). Interaction of oxygen gas with nonstoichiometric CeO_{2-x} was studied by measuring electrical conductivity as a function of oxygen partial pressure.

A number of different catalytic materials were studied: (i) microcrystalline cerium dioxide, (ii) nanocrystalline cerium dioxide, (iii) nanocrystalline nonstoichiometric cerium oxide, and (iv) various oxide supported metal catalysts. Cerium oxide is known for its propensity to reduction in the bulk phase at low oxygen partial pressure and high temperature. Microcrystalline ceria was used as a reference for nanocrystalline ceria in order to characterize bulk and surface reduction. The

nanocrystalline nonstoichiometric cerium oxide on the other hand was compared with the stoichiometric ceria to evaluate the effect of oxygen deficiency. Finally, doped or supported metal catalysts containing a second metal with the resulting additional degree of complexity were investigated.

EXPERIMENTAL

Microcrystalline CeO_2 (99.999%) was obtained from commercial sources (Heraeus). Nanocrystalline CeO_2 was prepared by calcination at 540°C for 4 h in air of cerium carbonate, which was precipitated from aqueous solutions of cerium nitrate and ammonium carbonate. Nanocrystalline nonstoichiometric CeO_{2-x} was synthesized by inert gas condensation. Metallic cerium was evaporated from a tungsten crucible in an atmosphere of 500 Pa helium. The metallic clusters were collected on a liquid nitrogen cooled substrate. After evaporating for 1 hour, the ultrahigh vacuum (UHV) chamber was evacuated and slowly back-filled with oxygen to a pressure of 1 kPa. The various metal oxide samples were used as powders in the catalytic, FT-IR, and TPR-studies. Only for the conductivity studies, a sample of nanocrystalline CeO_{2-x} was compacted to a porous self-supporting pellet at room temperature under 1 GPa uniaxial pressure. The specific surface areas were determined from B.E.T. analysis of nitrogen or krypton desorption isotherms to be 1, 58, and $75 \text{ m}^2/\text{g}$ for the microcrystalline CeO_2 , the nanocrystalline CeO_2 , and the nanocrystalline nonstoichiometric CeO_{2-x} , respectively. Doped or supported metal catalysts were either prepared by inert gas condensation [11], co-precipitation, impregnation or acquired from commercial sources (Heraeus).

Catalytic studies were performed in a packed bed reactor. The reactants were mixed, diluted in helium and passed over the catalysts (250 mg) in a quartz tube inside a tube furnace with a typical flow rate of $50 \text{ cm}^3/\text{min}$ and a contact time of 0.35 s. The gas compositions were 0.75% SO_2 / 1.5% CO diluted in He or Ar for catalytic oxidation of CO by SO_2 , and 1% CO / 5% O_2 diluted in He or Ar in the case of catalytic CO oxidation by O_2 . The effluent gas composition was continuously analyzed for reaction products by mass spectroscopy (Baltzers QMS64) as the temperature was raised at a constant rate.

In temperature programmed reduction measurements, a reducing gas mixture (20% H_2/Ar or 5% CO/Ar) was continuously passed over the catalyst while the temperature was increased at a constant rate. The effluent gas was analyzed by mass spectroscopy and the reduction of the sample was indicated by increasing concentration of the oxidized products. It is important to note, that the TPR experiment with CO is very similar to catalytic CO oxidation. The only difference is that oxygen is not present in the feed gas in the former but is supplied by the oxide catalyst itself. In other words, the reducing gas is probing the catalyst for oxygen that could be extracted. If oxygen species with different chemical activities were present in the catalyst, they would react with the reducing gas at different temperatures.

Infrared spectra were acquired using a Biorad FTS-60A spectrometer equipped with a diffuse reflectance cell (Harrick DRA3-HTC) allowing *in situ* measurements under reactive gas flow at temperatures up to 600°C . The metal oxide powders were mixed with KBr in a ratio of 1:1 in order to avoid specular reflections. The samples were pre-treated by purging the cell with 10%

O₂/He at temperatures between 200°C and 450°C until the signals due to water and the majority of surface hydroxyls were mainly suppressed.

The electrical conductivity of nanocrystalline nonstoichiometric CeO_{2-x} was measured using a QuadTech 7400 impedance analyzer. The real part of the impedance at a frequency of 10 Hz was measured as a function of oxygen concentration in the purge gas atmosphere.

RESULTS AND DISCUSSION

Stoichiometric CeO₂

Fig. 1a shows the activation profile for catalytic oxidation of CO by SO₂ over nanocrystalline stoichiometric CeO₂. Catalytic conversion was negligible below 500°C but increased rapidly at 560°C to 100% conversion. Fig. 2 exhibits the temperature programmed reduction of ceria in hydrogen for two samples with different specific surface areas. The high temperature peak at 800°C, which was found with both samples, indicated reduction of cerium oxide bulk phase. The additional peak at 580°C, which was observed with the high surface area sample only, could be assigned to reduction of the oxide surface. These results were in agreement with measurements by Yao et al. [12]. The coincidence of the surface reduction temperature, found in TPR and the catalytic activation temperature suggested that catalytic reduction of SO₂ by CO was rate-limited by the formation of oxygen vacancies at the surface. In this so-called interfacial redox mechanism [13], carbon monoxide continuously generated surface oxygen vacancies, whereas sulfur dioxide was reduced by donating oxygen to fill these vacancies.

The same stoichiometric CeO₂ catalyst was studied in catalytic CO oxidation by O₂. Activity was found at a much lower temperature of only 360°C (Fig. 1b). Based on the hydrogen-reduction

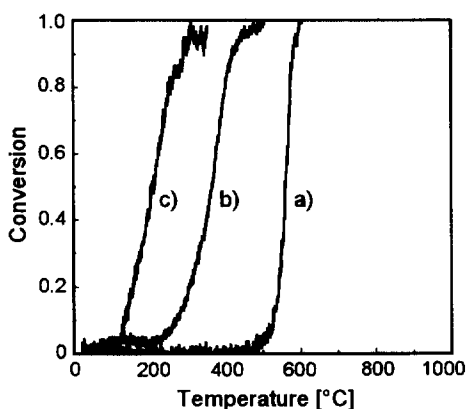


Fig.1. Catalytic conversion as function of reaction temperature with CeO₂ catalyst for CO oxidation by (a) SO₂ and (b) O₂ and with (c) CeO_{2-x} catalyst for CO oxidation by O₂.

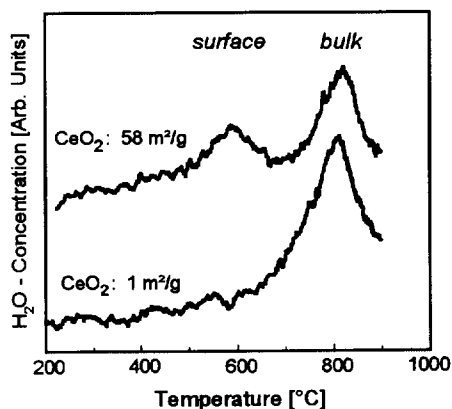


Fig.2. Hydrogen temperature programmed reduction of CeO₂ samples with high and low specific surface area as indicated.

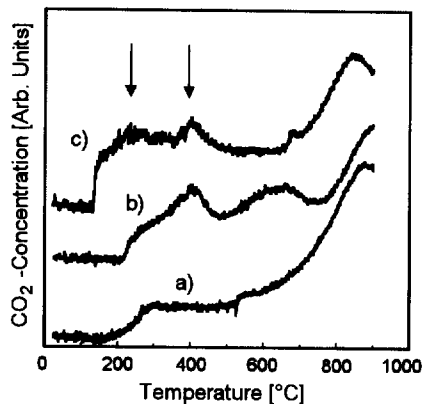


Fig.3. Carbon monoxide temperature programmed reduction of (a) microcrystalline CeO₂, (b) nanocrystalline CeO₂, and (c) nanocrystalline CeO_{2-x}.

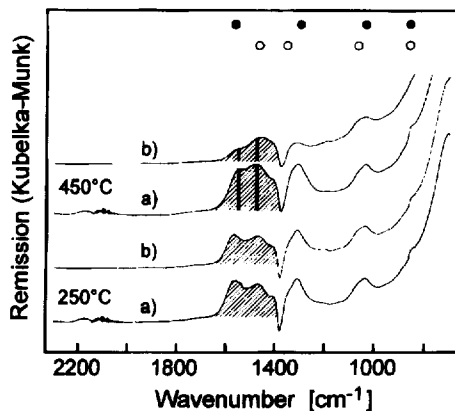


Fig.4. FT-IR spectra of nanocrystalline CeO₂ in (a) 10% O₂/He and (b) 2%CO/He at indicated temperatures. The peak positions of monodentate (open circles) and bidentate (closed circles) carbonates are also indicated.

measurements, one would not expect that oxygen vacancies were created at this low temperature at a sufficiently high rate necessary for a catalytic reaction.

Temperature programmed reduction measurements were also performed with CO as the reducing gas (Fig. 3). Similar to hydrogen TPR, bulk reduction was observed above 700 °C for both low and high surface area cerium dioxide. But contrary to hydrogen reduction, there were two additional peaks in the CO TPR spectrum of high surface area cerium oxide (Fig. 3b). The second peak starting at 500 °C with a maximum at 600 °C could be similar to the peak in H₂ TPR, associated with the formation of lattice oxygen vacancies at the surface. This also demonstrated that surface reduction was independent of the type of reducing gas. Furthermore, a low-temperature peak appeared at about 400 °C, which is similar to the sample's activation temperature for CO oxidation. The question arises whether there may be a low temperature reaction mechanism for CO oxidation that does not involve formation of oxygen vacancies, but is associated with a more reactive type of oxygen.

On metal oxides, CO adsorbs linearly on exposed metal cations, which have empty orbitals that accept the 5σ-lone electron pair at the carbon atom in an acid/base reaction. In addition and more extensively, CO chemisorbs by a redox reaction with surface oxygen to form CO₂ which can further react to surface carbonate, CO₃²⁻ [14]. Both linearly bonded CO as well as carbonates and carboxylates were detected on cerium oxide by infrared spectroscopy [15]. Linearly bonded CO was noted only below 100 °C, whereas the carbonates and carboxylates were found to be stable up to 500 °C. The most significant species were bidentate and monodentate carbonates. The carbonate with the lowest thermal stability is the bidentate carbonate, which is bonded to a metal cation via two terminating oxygen atoms. Above room temperature, the bidentate carbonate starts to transform into monodentate carbonate by cleavage of one of the two Ce-O bonds. The monodentate carbonate

is fairly stable and desorption was observed mainly between 300°C and 400°C.

In situ Fourier-transform infrared spectroscopy was employed to investigate the nature of chemisorbed carbon monoxide on the sample of this study. Fig. 4 shows four infrared spectra. The lower two were recorded at 250°C in diluted O₂ (a) and diluted CO (b) atmospheres. The positions of the two major carbonate species are indicated at the top of the graph. It is sufficient to focus on the two peaks at 1476 cm⁻¹ and 1577 cm⁻¹ as they are characteristic for monodentate and bidentate carbonate, respectively. Both bidentate and monodentate carbonate were found on the surface of this catalyst and little difference in total peak area was observed upon exposure to CO atmosphere vs. oxygen atmosphere at 250°C. The upper two plots in Fig. 4 show the spectra in diluted O₂ (a) and diluted CO (b) at a higher temperature of 450°C. Here, a clear decrease in the total peak area occurred when the sample was exposed to oxygen, and the decrease of intensity was larger for the bidentate carbonate than for the monodentate carbonate. These results were in complete agreement with the literature data [15] and suggested that CO oxidation on stoichiometric cerium oxide catalyst at 360°C proceeded by the following mechanism: carbon monoxide chemisorbed and reacted with low-coordinated terminating oxygen to form bidentate carbonate which was transformed to monodentate carbonate. The desorption of the monodentate carbonate between 300°C and 400°C [15] is suggested to be the rate-limiting step in CO oxidation.

Nonstoichiometric CeO_{2-x}

The activation of nonstoichiometric CeO_{2-x} catalyst for CO oxidation is shown in Fig. 1c. This cerium oxide material, synthesized by inert gas condensation, became active for CO oxidation at 200°C, which was 160°C lower than the activation or light-off temperature found for stoichiometric ceria catalyst.

Again, temperature programmed reduction with carbon monoxide was used to search for a signal indicating the presence of a correspondingly reactive oxygen species on the catalyst (Fig. 3c). A new peak, although fairly small, was observed at 250°C. The onset of this peak coincided with the catalytic activation for this nonstoichiometric material in CO oxidation reaction.

Recalling the particular importance of defects on chemisorption and catalytic properties, one might ask whether surface defects were present on nonstoichiometric CeO_{2-x} which caused the increased catalytic activity. Fig. 5 shows the infrared spectra measured *in situ* at 250°C in diluted 10% O₂/He for nanocrystalline CeO_{2-x} as prepared (a) and after oxidation for 1 hour at 450°C (b). We found additional peaks in the fresh sample, which disappeared after the sample had been oxidized at 450°C. These infrared peaks are also reported in literature for reduced cerium oxide [16] and are due to surface defects. Therefore, it could be assumed that the cerium oxide catalyst, generated by inert gas condensation did exhibit surface defects as expected, and that these surface defects were filled by oxidation at 450°C. If the low temperature CO oxidation mechanism were depending on these surface defects, the enhanced catalytic activity of nonstoichiometric cerium oxide should also vanish after oxidation at 450°C. The observation, however, is that the CO oxidation process at 200°C remains even after sample oxidation at 450°C (Fig. 6). This can only mean that surface defects, at least those giving rise to the infrared signals, are not the origin of the high CO oxidation catalytic activity.

CO temperature programmed reduction pointed to the presence of reactive oxygen which

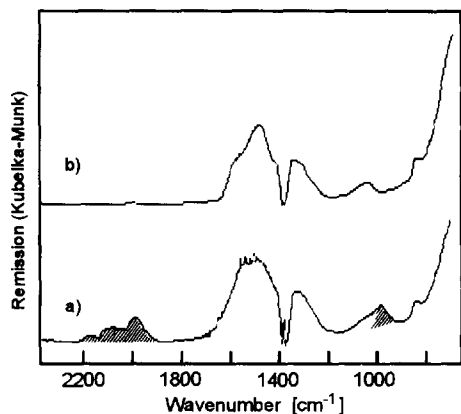


Fig. 5. FT-IR spectra of CeO_{2-x} (a) as prepared and (b) after oxidation for 1 hour at 450°C in $10\%\text{O}_2/\text{He}$. IR-signals due to surface defects are shaded.

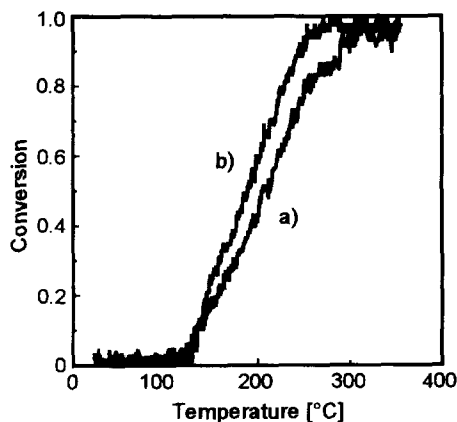


Fig. 6. Catalytic conversion in CO oxidation by O_2 for CeO_{2-x} catalyst (a) as prepared and (b) after oxidation for 1 hour at 450°C in $10\%\text{O}_2/\text{Ar}$.

might be chemisorbed oxygen. Chemisorption of oxygen on metal oxides is well described by the ionosorption model, due to the high electronegativity of oxygen [1]. The electron affinity of molecular oxygen in the gas phase is 0.45 eV which means that the capture of an electron is exothermic. Acquiring a second electron is not favorable in the gas phase but may occur on the surface of a solid. The unoccupied molecular orbitals of oxygen filled by these electrons are anti-bonding such that these peroxide ions tend to dissociate into singly ionized atomic oxygen. If the Madelung potential at the surface is high enough, this oxygen can accept a second electron to become fully ionized. This sequence is only hypothetical, it does not imply that these steps occur in this order. However, chemisorbed oxygen, especially the paramagnetic species O_2^- and O^- have been studied intensively by ESR. For a review on oxygen chemisorption on metal oxides, see [17]. The general result of these studies can be summarized as follows [14]:

1. Chemisorption of oxygen is low on defect-free surfaces of insulating metal oxides.
 2. The amount of chemisorbed oxygen increases with donor doping or surface defect concentration, both generating free electronic charge carriers.
 3. The degree of ionization ($\text{O}_2 \rightarrow \text{O}_2^{2-} \leftrightarrow \text{O}^-$) increases with defect concentration or electron density.
- These observations are the experimental basis for the ionosorption model which establishes a necessary condition that for chemisorption of oxygen, electrons need to be available in the solid for transfer from the solid to the oxygen.

The defect chemistry of cerium oxide is well established [18]. Oxygen deficiency in cerium oxide can be obtained by exposing the sample to low oxygen partial pressure at high temperature as seen in the TPR measurements. Upon reduction, oxygen is extracted from the lattice and escapes to the gas phase. In addition, a doubly ionized oxygen vacancy is left behind [18] and two electrons become mobile giving rise to electrical conductivity [19]. Electrical conductivity due to electronic

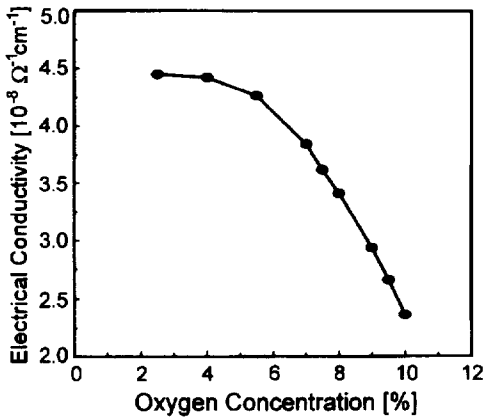


Fig.7. Electrical conductivity of nanocrystalline CeO_{2-x} as function of oxygen concentration in the gas phase at 230°C.

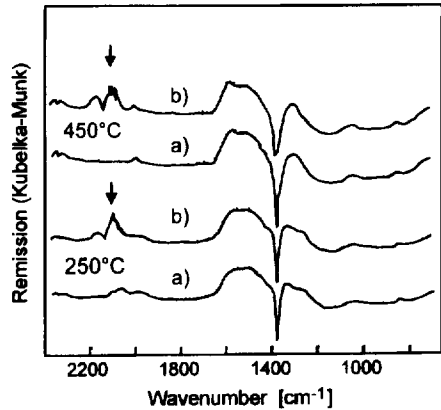


Fig.8. FT-IR spectra of Cu/CeO_{2-x} at 250°C and 450°C in (a) 10% O_2/He and (b) 2% CO/He . The IR-signal due to linearly bonded CO is indicated by arrows.

carriers is given by the product of electron mobility, charge and electron density. If these electrons, which are present in nonstoichiometric CeO_{2-x} , are extracted from the solid by chemisorbed oxygen, the electron density and consequently the conductivity will decrease. This effect could be observed with the nanocrystalline nonstoichiometric cerium oxide. Fig. 7 shows the electrical conductivity for nanocrystalline nonstoichiometric cerium oxide at 230°C. Electrical conductivity was found to decrease as oxygen partial pressure was raised indicating the trapping of electronic carriers by chemisorbed oxygen. Chemisorbed oxygen, particularly superoxide O_2^- ion, was also identified on pre-reduced cerium oxide by ESR and FT-IR [16,20,21].

The propensity to chemisorption of oxygen due to excess electrons, which are present in nonstoichiometric CeO_{2-x} , might promote catalytic CO oxidation at low temperature.

Supported metal catalysts

A number of different supported metal catalysts were investigated for catalytic activity in CO oxidation in order to obtain a basis for comparison for this reaction (Table 1). The most active commercial catalyst was 5% $\text{Pd}/\text{Al}_2\text{O}_3$ with a light-off temperature of 74°C. A very interesting and less expensive alternative to precious metals such as Pd or Pt is copper [10,22]. Different catalysts of Cu supported on metal oxide were investigated. Catalytic activity in CO oxidation by O_2 was found at temperatures as low as 68°C. Fig. 8 shows the FT-IR-spectra for Cu-doped nanocrystalline cerium oxide, generated by magnetron sputtering and inert gas condensation, which was catalytically active at 80°C. We observed a very strong additional signal at about 2100 cm^{-1} in 2% CO/He at 250°C. This peak was reversible even after oxidation of the catalyst at 450°C in oxygen, and was due to carbon monoxide, linearly adsorbed on exposed Cu atoms. For supported metal catalysts, a new aspect needs to be considered in the mechanism. In the case of undoped cerium oxide catalysts, catalytic activity was related to chemical activity of the oxygen that was

TABLE 1

Light-off Temperatures in Catalytic CO Oxidation by O₂ for Various Supported Metal Catalysts.

Catalyst	Synthesis and pre-treatment	CO oxidation by O ₂ light-off temperature
Pd/Al ₂ O ₃	commercial (Heraeus), oxidized at 300°C in 2%O ₂	74°C
Pt/Al ₂ O ₃	commercial (Heraeus), oxidized at 300°C in 2%O ₂	111°C
Cu/TiO ₂	impregnated, oxidized at 300°C in 2%O ₂	113°C
Cu/CeO ₂	mechanically mixed, oxidized at 300°C in 2%O ₂	117°C
Cu/CeO ₂	impregnated, oxidized at 300°C in 2%O ₂	68°C
Cu/CeO _{2-x}	magnetron sputtering, inert gas condensation	80°C

present on the catalyst. Transition metals supported on metal oxides provide surface sites for linearly bonded highly active carbon monoxide. This chemisorbed CO may react with oxygen, which is either chemisorbed on the metal or on the metal oxide.

SUMMARY

Nanocrystalline nonstoichiometric CeO_{2-x} was synthesized by inert gas condensation and post-oxidation. Surface chemical reactivity of this material was compared with stoichiometric nanocrystalline and microcrystalline CeO₂. The light-off temperatures of catalytic redox reactions, the oxidation of CO by SO₂ and O₂, were determined. Temperature programmed reduction was employed to probe the catalyst surface for different types of oxygen that could be distinguished by their chemical activity. Various TPR signals were found and could be associated with the activation of different catalytic reactions. This correlation in activation temperature suggested three different reaction mechanisms. Catalytic oxidation of CO by SO₂ using CeO₂ catalyst required the highest reaction temperature (580°C), and involved the formation of surface oxygen vacancies. CO oxidation by O₂ on the same catalyst was observed at 360°C, and was rate-limited by the desorption of surface carbonate. Nonstoichiometric CeO_{2-x} catalyst showed high activity for CO oxidation at 200°C which could be related to the presence of chemisorbed oxygen. Catalytic activity of supported metal catalyst at temperatures below 100°C was related to the presence of highly active chemisorbed CO, which was linearly adsorbed on the metal surface.

ACKNOWLEDGMENT

The authors wish to thank Eric Sommer and Tao Sun for their helpful discussions and technical assistance with electrical conductivity and FT-IR measurements. Financial support by the NSF (CTS-9257223, DMR-9400334) and DFG (SFB 277) is acknowledged.

References

1. S.R. Morrison, *The Chemical Physics of Surfaces*, 2nd Ed., Plenum Press, New York (1990).
2. R.W. Siegel and H. Hahn, *Current Trends in Physics of Materials* (M. Yussouff, Ed.), World Scientific Publ. Co., Singapore, p. 403 (1987).
3. J. Karch, R. Birringer, and H. Gleiter, *Nature* **330**, 556 (1987).
4. R.S. Averback, H. Hahn, H.J. Höfler, J.L. Logas, and T.C. Chen, *Materials Research Society Symposium Proceedings*, **153**, p. 3, Mater. Res. Soc., Pittsburgh, PA (1989).
5. D.D. Beck and R.W. Siegel, *J. Mater. Res.* **7** [10] 2840 (1992).
6. H.W. Sarkas, S.T. Arnold, J.H. Hendricks, L.H. Kidder, C.A. Jones, and K.H. Bowen, *Z. Phys.* **D26** 46 (1993).
7. H.-M. Lin, C.-Y. Tung, C.-M. Hsu, and P.-Y. Lee, *J. Mater. Res.* **10** [5] 1115 (1995).
8. A. Tschöpe, J.Y. Ying, *Nanophase Materials*, (G.C. Hadjipanayis and R.W. Siegel, Eds.) p. 781, Kluwer Academic, Dordrecht/Norwell, MA, 1994.
9. A. Tschöpe, J.Y. Ying, W. Liu, and M. Flytzani-Stephanopoulos, *Materials Research Society Symposium Proceedings*, **344** p. 133, Mater. Res. Soc., Pittsburgh, PA (1995).
10. A. Tschöpe, W. Liu, M. Flytzani-Stephanopoulos, and J.Y. Ying, *J. Catal.* **157** 42 (1995).
11. A. Tschöpe and J.Y. Ying, *Nanostr. Mater.* **4** [5] 617 (1994).
12. H.C. Yao and Y.F. Yu Yao, *J. Catal.* **86** 254 (1984).
13. A. Bielanski and J. Haber, *Oxygen in Catalysis*, Dekker, New York (1991).
14. V.E. Henrich and P.A. Cox, *The Surface Science of Metal Oxides*, Cambridge Univ. Press, Cambridge, p. 257 (1994).
15. C. Li, Y. Sakata, T. Arai, K. Domen, K. Maruya, and T. Onishi, *J. Chem. Soc. Faraday Trans.* **85** [4] 929 (1989).
16. C. Li, K. Domen, K. Maruya, and T. Onishi, *J. Am. Chem. Soc.* **111** 7683 (1989).
17. M. Che and A.J. Tench, *Adv. Catal.* **32**, 1 (1983).
18. H.L. Tuller and A.S. Nowick, *J. Electrochem. Soc.* **126** 209 (1979).
19. H.L. Tuller and A.S. Nowick, *J. Phys. Chem. Sol.* **38** 859 (1977).
20. M. Che, J.F.J. Kibblewhite, A.J. Tench, M. Dufaux, and C. Naccache, *J. Chem. Soc. Faraday Trans.* **69** [1] 857 (1973).
21. X. Zhang and K.J. Klabunde, *Inorg. Chem.* **31** 1706 (1992).
22. A. Tschöpe, J. Ying, and Y.-M. Chiang, *Mater. Sci. Eng.* **A204** 267 (1995).